BAUET JOURNAL
Published by
Bangladesh Army University of Engineering & Technology (BAUET)
Journal Homepage: https://journal.bauet.ac.bd/
DOI: https://doi.org/10.59321/BAUETJ.V5I1.5

Effect of Blade Number and Angle of Attack on the Performance of a Horizontal Axis Tidal Current Turbine: A Numerical Study

Md. Mezbah Uddin[1*], Kazi Rafi Rahaman[1], Md. Thanvir Islam[1], Tasmia Hoque[1], S M Ikhtiar Mahmud[1]

[1]Department of Naval Architecture and Marine Engineering, Military Institute of Science and Technology, Mirpur Cantonment, Dhaka-1216, Bangladesh

Abstract: Power generation from tidal currents is gaining attention because it is predictable and produces zero CO_2 emissions. A tidal turbine works similarly to a wind turbine, converting sea current energy into power. Turbines are classified by blade orientation: horizontal axis, vertical axis, and helical variants. Among these, horizontal axis tidal current turbines (HATCT) offer higher efficiency due to their lift-based design. This study uses numerical analysis to examine HATCT blades with different numbers of blades and varying angles of attack, applying Blade Element Momentum (BEM) theory and Computational Fluid Dynamics (CFD). Tidal turbine blade models were created in SOLIDWORKS and analyzed in ANSYS to evaluate torque and power output under different design conditions. In this investigation, the major design parameters considered include the angles of attack of 10°, 20°, and 30°, the number of blades from 2 to 4, and the tip speed ratio (TSR), all of which significantly influence the turbine's hydrodynamic performance. Flow velocity and coefficient of power (CP) were also examined to assess the overall performance. The results revealed that the 3-bladed turbine at 30° angle of attack achieved the highest efficiency, producing 2.79 MW of power with a power coefficient of 0.47.

Keywords: *Tidal Current; Horizontal Axis; Angle of attack; Blade Element Moment; Tip Speed Ratio*

Introduction: Nowadays, the demand for power is increasing day by day. As a consequence, there are lots of research works ongoing for new and better ways to produce electricity. The global reliance on fossil fuels is significant, as seen by the fact that coal, oil, and natural gas account for 72% of the total electricity market share. This heavy consumption of fossil fuels is driven by a growing energy demand, leading to a substantial portion of the world's energy needs being fulfilled through it. The escalating emphasis on fossil fuels has emerged as a significant cause for concern. The usage of fossil fuels for energy generation has been determined to have adverse effects on the environment, such as the emission of greenhouse gases and the amplification of global warming. The implications possess the capacity to precipitate significant environmental crises. Consequently, nations across the globe have recognized the necessity of integrating renewable energy sources into their energy strategies as a viable substitute for fossil fuels.

Renewable energy encompasses a variety of technologies, such as geothermal, solar, wind, and wave energy, which harness energy from surroundings with minimal negative effects in comparison to traditional energy sources. Currently, there is a significant amount of research and development dedicated to the exploration of renewable energy sources as a viable alternative to the combustion of fossil fuels. Ocean waves and currents are significant sources of energy that can be harnessed by humanity to fulfill their energy requirements, thereby capitalizing on the associated knowledge and advantages. The utilization of renewable energies leads to a decrease in the consumption of fossil fuels, and they can be employed selectively to fulfill certain requirements, so conserving fossil fuel resources. The adoption of this strategy will help protect the environment against the adverse impacts of the release of greenhouse gases and industrial effluence generated by the usage of fossil fuels. Additionally, it will facilitate the harnessing of renewable energy sources, thereby ensuring a sustainable and abundant supply of natural energy. In his master's thesis, Nazari conducted a comprehensive examination of several kinds of maritime renewable energy. Subsequently, the individual proceeded to develop a point absorber energy system specifically tailored for use in the Persian Gulf [1,2]. From a geometric and physical perspective, tidal turbines and wind turbines exhibit notable similarities. Consequently, aerodynamic and hydrodynamic characteristics exhibit a high degree of similarity. Tidal turbines, akin to wind turbines, can be grouped into two primary classifications: vertical-axis turbines and horizontal-axis turbines. The efficiency of horizontal-axis turbines is often regarded as superior to that of vertical-axis turbines, mostly because of their use of a lifting force mechanism. The attribute has led to a reduction in the usage of vertical-axis turbines.

Most tidal current turbines (TCTs) in China are still in the hundred-kilowatt range. For example, in 2016, LHD developed modular vertical-axis turbines, including two 300 kW and two 200 kW units. Harbin Engineering University's Haineng III system consists of two 300 kW vertical-axis turbines. Zhejiang University has also conducted sea trials with 60 kW and 120 kW horizontal-axis turbines [3-5]. Key design goals for standalone TCTs include achieving high efficiency, minimizing mechanical loads, and preventing cavitation. Previous research has focused on optimizing blade designs and control algorithms

Article history:
Received: 25 June 2025
Received in revised form: 10 August 2025
Accepted: 10 November 2025
Available online: 15 December 2025

Corresponding author details: Md. Mezbah Uddin
E-mail address: mezbah@name.mist.ac.bd
Tel: +8801712794447

Copyright © 2025 BAUET, all rights reserved

to maximize power output [6,7]. However, advanced control strategies often require precise system modeling and high-performance controllers. TCTs also face challenges from complex marine environments, such as unsteady flows and wave interactions, which significantly affect blade loading and performance [8-10]. Additionally, theoretical studies have explored turbine array configurations and optimization [11-14], with large-scale deployment depending heavily on reducing the cost of individual TCT units.

Tidal energy exhibits notable advantages in comparison to wind energy, mostly due to its heightened predictability. Numerical approaches and experimental measurements were employed by numerous researchers to investigate the performance of tidal turbines. Power and thrust in sea current turbines under varied hydrodynamic flow conditions were measured by Bhaj et al [15]. This experiment was conducted in a towing tank as well as a cavitation tunnel. Numerical methodologies are utilized to facilitate the design and forecast the operational efficacy of maritime turbines and propellers [16]. In their study, Shi et al. utilized ANSYS CFX software to investigate the hydrodynamic properties of a three-bladed tidal turbine and its efficiency in the presence of flow separation [17]. The numerical methodology utilized for the examination of the three-blade tidal turbine by computational fluid dynamics (CFD) [18].

During the time period 2002 to 2012, research on horizontal-axis tidal current turbines (HATCTs) focused heavily on turbine performance, wake interactions, generator integration, and environmental impacts. A decade of progress was reviewed by Ng et al. [19], highlighting the growing technical maturity and economic potential of these systems. Since then, research has shifted toward advanced design strategies aimed at maximizing performance. Innovations such as adaptive, variable-pitch blades have improved hydrodynamic efficiency and enabled bidirectional energy capture, while diffuser-augmented designs have enhanced power output [20]. Studies on wake behavior and fluid-structure interactions have also informed better array layouts and overall farm efficiency [21]. Large-scale deployments like Raz Blanchard in France and the MeyGen project in Scotland mark a transition toward commercial viability. These projects demonstrate that improved efficiency, reliability, and reduced maintenance can make HATCTs a practical energy solution for coastal and island regions [22]. Ongoing advancements in environmental integration, control systems, and blade design continue to reinforce tidal energy's role in the global renewable energy portfolio.

Numerous systems have recently been developed to generate electricity from tidal currents [23]. Horizontal-axis tidal current turbines (HATCTs), also known as axial flow turbines, operate with their rotational axis aligned parallel to the tidal flow and are designed to function in a single flow direction. Their operating principle is similar to that of horizontal-axis wind turbines (HAWTs). Advances in computing power and computational fluid dynamics (CFD) have significantly improved the ability to model the complex flow around these turbines [24]. In the context of Bangladesh, deploying tidal current turbines presents a promising opportunity. With an extensive coastline along the Bay of Bengal and numerous tidal rivers, the country holds substantial potential for tidal energy harvesting. Installing horizontal-axis tidal turbines offers a practical method to tap into this resource. To ensure optimal performance and design adaptation to local tidal conditions, CFD analysis is essential. Given its predictability and reliability, tidal energy stands out as a viable alternative to fossil fuels for Bangladesh. HATCTs aim to convert the kinetic energy of tidal currents into electricity, functioning much like underwater wind turbines [25].

Noruzi et al. [26] conducted a study that centered on the design, analysis, and evaluation of the performance of a horizontal marine stream axial turbine. The researchers specifically considered the impact of turbine installation depth on its hydrokinetic characteristics. In order to represent the significant magnitude of ocean waves, the researchers employed the linear wave theory to analyze gravity waves. The simulation of the tidal turbine's actuator disc theory was conducted [27]. The present study involves a comparative analysis of various turbulence models employed for simulating the wake characteristics behind a turbine, which is represented by a porous disc. The models that underwent testing included the Standard and realizable k-ε models, the SST k-ω model, and the Reynolds stress model (RSM). The density disparity between seawater and wind results in the tidal current turbine yielding significantly higher energy output compared to the wind turbine. The utilization of tidal currents as a renewable energy resource is predicated on the conversion of the kinetic energy inherent in the movement of water into mechanical power, which in turn drives generators via the implementation of tidal turbines. The technology under consideration exhibits a complete absence of carbon dioxide emissions, thereby offering a potential solution to the issue of dependence on fossil fuels [28].

A numerical investigation on the hydrodynamic performance of a horizontal-axis tidal current turbine has been performed using the Reynolds Stress Turbulence model in STAR-CCM+. It found that lift increases more linearly than drag with the angle of attack until a critical point. Power and torque coefficients have risen with tip speed ratio (TSR), peaking at TSR 5. Compared to the k-ε model, the Reynolds model yielded higher performance, with actual turbine power (0.9145 MW) falling short of theoretical estimates (1.1297 MW) [29]. An investigation used CFD simulations to evaluate a horizontal axis tidal current turbine (HATCT) under site-specific conditions in the Passur River, Bangladesh. Results showed consistent thrust, torque, and power outputs across different mesh resolutions, confirming numerical stability. The turbine generated approximately 3 kWh per tidal cycle, demonstrating its potential for localized renewable energy. The findings support the feasibility of deploying HATCTs in estuarine environments for sustainable power generation [30]. Chen et al. [31] have designed and analyzed a 100-kW horizontal axis tidal current turbine (HATCT) suitable for shallow coastal waters using Blade Element Momentum Theory and CFD. The NACA63-415 airfoil showed strong aerodynamic performance, achieving a peak power coefficient (Cp) of 0.467 at TSR 7. Radial flow and blade tip design significantly influenced efficiency, with reduced tip chord length lowering Cp but offering material savings. The study presented the design, numerical simulation, and experimental validation of a horizontal-axis tidal current turbine optimized for a 300-kW output. Using modified blade element theory and custom airfoils to prevent cavitation, the turbine achieved a peak efficiency of 45% at a tip speed ratio (TSR) of 3.5. Experimental towing tank tests confirmed strong performance across a range of TSRs (3-5), validating the design approach [32]. A 600-kW horizontal-axis tidal current turbine was designed, tested onshore, and successfully deployed in a sea trial in Zhoushan, China. The turbine, featuring a two-blade rotor and a semi-direct-drive system, achieved a high-power coefficient (Cp = 0.385), close to its theoretical maximum (0.396). Sea trials confirmed stable MPPT control and efficient energy capture, though power fluctuations were observed due to stream shear. The study demonstrated the turbine's reliability and provides a reference for future large-scale TCT development [33].

Despite the availability of advanced CFD tools and the theoretical advantages of horizontal-axis tidal current turbines (HATCTs), their application in Bangladesh remains limited. Estuarine regions like the Meghna River offer significant tidal energy potential, yet localized performance data and design optimization tailored to the country's unique hydrodynamic conditions are lacking. Much of the existing research relies on generalized models or offshore scenarios, often overlooking the specific characteristics of Bangladesh's tidal zones. This study addresses that gap by using CFD analysis to evaluate the performance of HATCTs in the Meghna River near Sandwip Island under site-specific conditions. The research focuses on the numerical analysis of turbine blades, examining variations in blade number and angle of attack. Blade design was carried out using SOLIDWORKS, and performance simulations were conducted in ANSYS CFX, a high-performance CFD platform. The analysis involved simulating fluid flow across turbine blades to calculate torque and assess power output across different design configurations, ultimately identifying improvements in turbine efficiency.

Methodology:

a) Hydrodynamics Basis: Angle of Attack (AOA) and Hydrofoil Section: The analysis is grounded in the angle of attack (AOA), defined as the angle between the hydrofoil chord line and the relative flow vector. A NACA airfoil (taken from the web), commonly used in tidal turbine blade design, as shown in Fig. 1, illustrates the AOA with respect to the chord line and the incoming flow. In this study, AOA = 10°, 20°, and 30° were investigated to assess their impact on turbine performance.

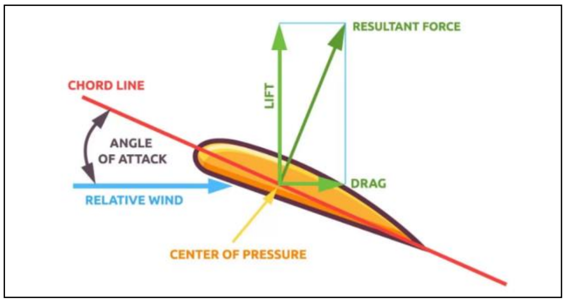

Fig. 1: Angle of attack of turbine hydrofoil.

A hydrofoil is a two-dimensional surface that operates in water, producing a lift force. In this study, a hydrofoil was selected for the purpose of varying the angle of attack, along with the variation in the number of blades. In this study, the SG-6043 hydrofoil was selected, which is specially designed for low Reynolds numbers. SG 6043 has a maximum camber of 5.1% at 53.3% of the chord and a maximum thickness found at 10% at 32.1% of the chord, which results in a high lift ratio; hence, the power capabilities are optimal at a low speed [34]. The hydrofoil's shape results in a disparity in flow velocity between the upper and bottom surfaces, with the former experiencing higher velocities. The disparities give rise to a variation in pressure, whereby pressure exhibits an inverse relationship with velocity. The relationship between force and pressure can be expressed as the product of pressure and area, indicating that pressure is a determinant of force. The desired force, known as the lift force (Lf), is oriented perpendicularly to the direction of the stream flow. The drag force (D_f) is a parasitic force that acts parallel to the direction of the stream flow. The power production of tidal turbines is determined through the calculation of tangential force, considering the effects of lift and drag forces. These relationships can be expressed mathematically using the following equations:

Lift force: $L_f = \frac{1}{2}\rho V^2 A C_L$ eq. 1

Drag force: $D_f = \frac{1}{2}\rho V^2 D C_D$ eq. 2

Reynolds number: $R_e = \frac{\rho V x}{\mu}$ eq. 3

Lift coefficient: $C_L = \frac{Lf}{\frac{1}{2}\rho V^2 A}$ eq. 4

Drag coefficient: $C_D = \frac{Df}{\frac{1}{2}\rho V^2 A}$ eq. 5

The total amount of theoretical power from water P_a that can be extracted from a tidal stream is dependent on the stream's velocity v, the fluid's density, and the blade's swept area S. It can be expressed as:

$$P_{tidal\ stream} = P_a = 0.5\,\square SV^3 \qquad \text{eq. 6}$$

$$P_e = T_{turbine}\,\square = nT_{blade}\,\square \qquad \text{eq. 7}$$

The Coefficient of Power (C_P) is defined as the ratio of P_a to P_e

$$C_P = \frac{P_a}{P_e} \qquad \text{eq. 8}$$

This is considered to be the fundamental determinant of the efficiency of a turbine. It is typically graphed in relation to the ratio of the tip speed (TSR). This ratio is expressed as the relation between the blade tip's tangential speed and the actual fluid flow velocity, as shown in the following equation:

$$TSR = \frac{\omega D}{2V} \qquad \text{eq. 9}$$

Despite the extensive application of the Boundary Element Method (BEM) in the design and analysis of tidal turbines, which is backed by experimental and numerical comparisons, additional support is needed when utilizing this approach to investigate particular aspects of tidal turbine hydrodynamics. These issues encompass the evaluation of forces exerted on the blade, the characterization of flow over the blade, and the understanding of flow phenomena within the blade sections [25]. CFD is a powerful tool that, when used either singly or in conjunction with other simulation tools, can provide detailed information about the local flow and hence performance of a marine current turbine in varying flow conditions [35]. The following Table 1 represents the geometrical characteristics of the hydrofoil SG-6043.

Table 1. Geometrical characteristics of the hydrofoil SG-6043.

SG 6043			
x/c	**y/c**	**x/c**	**y/c**
1.00000	0.00000	0.25633	0.09491
0.99811	0.00066	0.22567	0.09127
0.99274	0.00271	0.19645	0.08702
0.98439	0.00607	0.16882	0.08220
0.97343	0.01047	0.14293	0.07884
0.96007	0.01552	0.11890	0.07100
0.94429	0.02092	0.09687	0.06473
0.92597	0.02655	0.07694	0.05809
0.90516	0.03248	0.05920	0.05117
0.88207	0.03868	0.04376	0.04398
0.85688	0.04510	0.03062	0.03859
0.82979	0.05165	0.01983	0.02918
0.80101	0.05824	0.01142	0.02171
0.77074	0.06478	0.00528	0.01436
0.73922	0.07114	0.00150	0.00741
0.70666	0.07717	0.00002	0.00094
0.67320	0.08268	0.00059	-0.00468
0.63889	0.08761	0.00393	-0.00660
0.60396	0.09190	0.84468	0.01592
0.56854	0.09551	0.87567	0.01447
0.53276	0.09842	0.90377	0.01265
0.49685	0.10059	0.92871	0.01056
0.46096	0.10201	0.95024	0.00828
0.42528	0.10269	0.96814	0.00591
0.39000	0.10260	0.98215	0.00361
0.35527	0.10175	0.99209	0.00170
0.32131	0.10017	0.99803	0.00045
0.28827	0.09788	1.00000	0.00000

b) Turbine Parameterization and Site Conditions: The horizontal-axis tidal current turbine (HATCT) is based on the SG-6043 section and parameterized for a Meghna River site near Sandwip Island, where the peak stream velocity is V=5 m [36]. Table 2 presents the turbine key design and operating specification. This design is mainly focused on the consequences of accounting for various angles of attack (10, 20, 30 degrees) and on the influence of changing the number of blades from n=2 to n=4. Various interconnected factors, including the blade profile, blade tip losses, angle of attack, and rotor rotational speed, influence the prediction of the hydrodynamic performance of the HATCT. Furthermore, the performance of the turbine is influenced by flow conditions, including average free-stream velocity, namely the incidence flow speed, and the presence of freestream turbulence. According to a non-dimensional similarity analysis, the dominant factors influencing the overall performance of these turbines may be attributed to three specific quantities. The Reynolds number (Re), tip speed ratio, and number of blades are important parameters in the study of fluid dynamics and aerodynamics. These variables play a significant role in the analysis and design of various engineering systems, particularly those involving fluid flow and rotating machinery. The Reynolds number characterizes the flow regime and determines the relative importance of inertial and viscous forces. The tip speed ratio relates the rotational speed of a device to the velocity of the fluid it interacts with, providing insight into the efficiency. It is necessary to meticulously consider and analyze the impacts of each of these variables in order to cultivate a comprehensive comprehension of the hydrodynamic flow and its behavior. The optimization of the number of blades and TSR is crucial, as it is influenced by the inlet flow conditions. A higher number of blades is often linked to a lower TSR, resulting in reduced efficiency as a result of blade halting at higher flow incidence. On the other hand, it should be noted that a higher TSR is associated with a decline in the lift coefficient due to a fall in the angle of attack, hence resulting in a reduction in overall efficiency.

Table 2. Turbine specific design parameters.

Design Parameters	Specification
Primary Blade Hydrofoil	SG-6043
Approximate Location	Near Sawndip Island, Meghna river
Inlet velocity	5 m/s
Rotor diameter	11.1 m
Blade Length	5 m
Hub diameter	1 m
Hub height	12 m
Water Depth	20 m
Number of Blades	2,3,4
Angle of Attack	10,20,30 degrees

HATCTs are shown in Fig. 2, which were designed through advanced solid modeling design software-SOLIDWORKS, with an optimal angle of attack that maximizes both lift and the lift-to-drag ratio, resulting in the highest power output for tidal turbines.

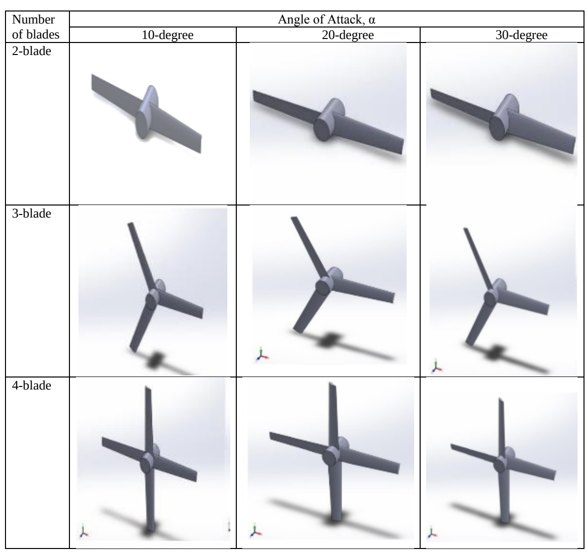

Fig. 2: 3-D modeling of design turbine.

c) Numerical model: The numerical study selected for developing a designed model of HATCT involves the selection of a hydrofoil using the ANSYS CFX modeler. A comprehensive computational fluid dynamics (CFD) investigation was conducted utilizing a turbulence model titled as Shear Stress Transport (SST) at low-order k-ω in order to assess the efficacy of horizontal axis tidal current turbines (HATCTs) with respect to various parameters, including angle of attack (AOA), ratio of the tip speed (λ) and blade number (n). Rotational speed of rotor (ω) using tip speed ratio $\lambda = \frac{\omega D}{2V}$, where D is the rotor diameter. This initial parameter proposed for the analyses shown in Table 3 and Table 4.

Table 3. Initial parameter settings in ANSYS.

TSR (λ) Range	
2-BLADE	7-8
3-BLADE	5-6
4-BLADE	3-4

Table 4. Parameter settings in ANSYS.

Number of blades	Angle of Attack	Tip speed ratio λ	Rotational speed ω (rpm)	Relative pressure p (kPa)
2-blade	10-degree	7.2	61.93	190
	20-degree	7.5	64.51	190
	30-degree	7.8	67.10	190
3-blade	10-degree	5.7	49.46	190
	20-degree	6.4	55.57	190
	30-degree	6.7	58.15	190
4-blade	10-degree	3.3	28.39	190
	20-degree	3.6	31.23	190
	30-degree	4.2	36.38	190

d) Computational Domain, Meshing and Boundary Condition: The fluid domain comprises two coaxial cylindrical enclosures as shown in Fig. 3. Enclosure 1: rotor vicinity and fluid-structure interaction interface. Enclosure 2: outer computational boundary (inlet, outlet, walls), with interfaces 1–3 connecting hub/blade regions.

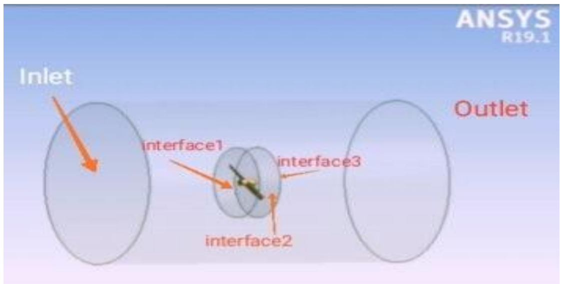

Fig. 3: Different regions of the confined boundary.

Meshing is a crucial component of the modeling and simulation procedure; wherein intricate geometries are partitioned into elementary parts that serve as discrete or local approximations of the broader domain. A range of methods are available that encompass several types of meshing, including high-order and linear components, as well as rapid tetrahedral and polyhedral methods, and high-quality hexahedral and Mosaic methods. Several mesh types include triangular, quadrilateral, tetrahedral, hexahedral, pyramid and prism (wedge) among these hybrids meshing tetrahedral, pyramid and prism (wedge) and hex dominant mesh are cut shell. For this analysis, mesh specifications are mentioned in a brief in the following Table 5 and shown in Fig. 4. Moreover, global meshing settings were fixed as well as physics preference was stated as CFD, and solver preference was CFX. The size of element predefined within 100 mm up to maximum size 200mm. The mesh sensitivity analysis and mesh metrics were verified prior to conducting the simulation as shown in Fig. 5 and Fig. 6.

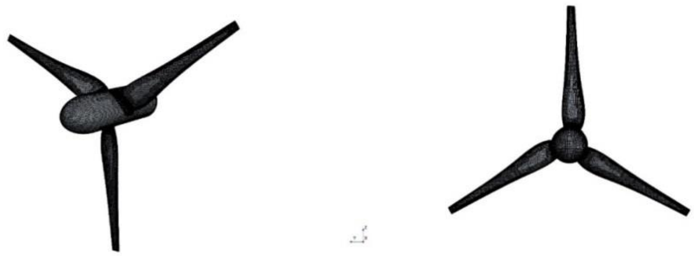

Fig. 4: 3-bladed turbine after meshing.

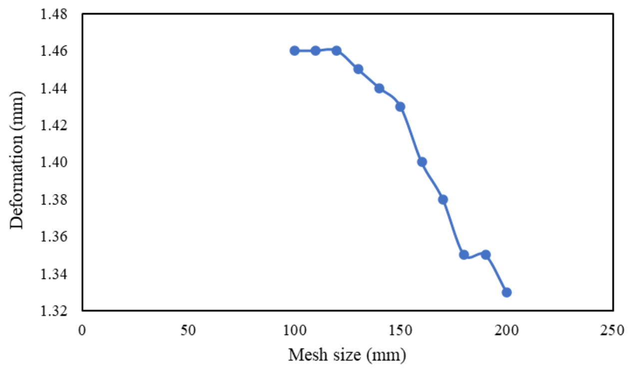

Fig. 5: Mesh convergence.

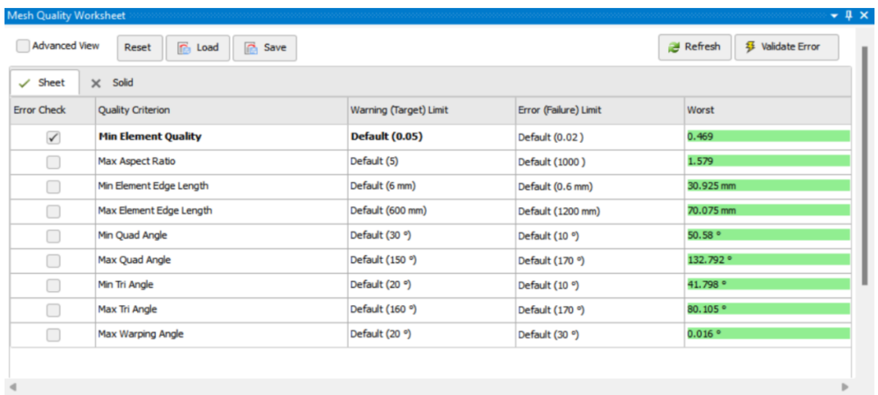

Fig. 6: Mesh metrics.

Table 5. Mesh specifications.

Mesh Specifications	
Blade diameter	11.1
Total number of nodes	320150
Total number of elements	586522

The analytical solutions investigated for torque and various angle of attack which are 10°, 20°, 30° according to number of blades. This numerical experiment based on the projection of tidal turbine in the MEGHNA river where the flow velocity considering 5m/s. In this flow velocity the analyses set for 500 iterations having the picture of torque upon the tidal turbine as represented by Fig. 7.

The present investigation applied a turbulence model referred to as SST (Shear Stress Transport) at low-order k-ω to analyze the impact of angle of attack, ratio of tip speed and blade number on the performance of HATCTs in terms of power coefficient. CFD setup details, including turbulence intensity, study type, and solver settings, are summarized in Table 6.

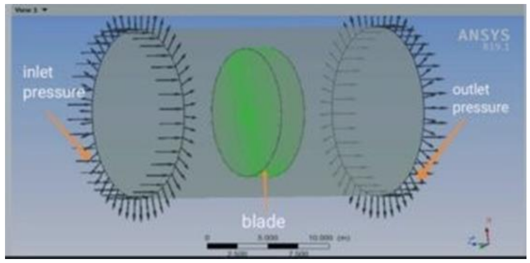

Fig. 7: Flow setting applied on the confined boundary region.

Table 6. Boundary conditions and simulation setup.

Parameter	Specification
Study type	Steady state simulation
Solver	ANSYS CFX (CFD)
Turbulence model	SST k-ω
Solver	5% at inlet
Fluid	Water ($\rho = 1000\ kg/m^3$, □ = 0.001 Pa·s)
Inlet velocity	5 m/s
Outlet velocity	Static pressure = 0 Pa
Wall condition	No slip on blade and hub surface
Interfaces	Enclosure 1 and 2 (rotor fluid interaction)
Simulation Iterations	500
Convergence Criteria	Residuals ≤ 10^{-4}

Results and Discussion: At first the value of the tidal stream power also known as an incoming stream power for tidal turbine, which calculated 5.939398 MW using its formula is $P_{tidal\ stream} = P_a = 0.5\rho SV^3$ where $A = \pi \times R^2$ and density of water used as 1000 kgm^{-3}. After analyses, obtained the value of torque and having the value of power P of turbine. Finally, power of coefficient C_P calculated from the ratio of turbine power P to tidal stream power $P_{tidal\ stream}$. In Table 6 shows the torque getting from ANSYS analyses as well as the power of coefficient. The maximum power was at 30degree angle having 1.96 MW, which had greater power coefficient 0.33. In case for blade number 3, the maximum power 2.79 MW at angle 30 degree as well as the power of coefficient 0.47 and in case for blade number 4, the maximum power 2.07 MW at angle 30 degree as well as the power of coefficient 0.34. A typical representation of the velocity pattern after analysis in a 3-bladed turbine at 30° AOA is illustrated in Fig. 8.

Fig. 8: 3-bladed turbine after analysis.

These results indicate that increasing the angle of attack enhances the lift generated by the hydrofoil until 30°, resulting in greater torque and power output. Beyond this angle flow separation is likely to occur which can cause deterioration of the performance of the turbine. Similarly, increasing the number of blades improves the torque due to a larger effective area interacting with the fluid, however, excessive blade count increases drag and reduces rotational speed and limits the overall efficiency. The overall result from the simulation has been compiled in Table 7.

Table 7. Power and torque obtained at different AOA.

.	Angle of Attack	Torque, T (kgm²/s2)	Power, P (MW)	Power of tidal stream Ptidal stream (MW)	Coefficient of Power CP
2-blade	10-degree	274548	1.79	5.93	0.30
	20-degree	272772	1.85	5.93	0.31
	30-degree	276445	1.96	5.93	0.33
3-blade	10-degree	447174	2.31	5.93	0.39
	20-degree	449026	2.61	5.93	0.43
	30-degree	458377	2.79	5.93	0.47
4-blade	10-degree	514747	1.54	5.93	0.25
	20-degree	526735	1.72	5.93	0.29
	30-degree	544185	2.07	5.93	0.34

From Table 7 it is evident that torque consistently increases with both blade number and angle of attack. However, the trend in power coefficient reveals that higher blade counts do not always yield higher efficiency since increased drag at four blades offsets the torque advantage. Therefore, the 3-blade turbine at 30° provides the optimal performance, balancing torque, power and hydrodynamic efficiency. This comparison is based on the parameters namely TSR (λ), blade number and angle of attack. To enhance the efficiency of HATCT, a thorough analysis of many non-dimensional parameters, including ratio of the tip speed, blade's number, and Reynolds number, is required.

a) **Power-TSR relationship:** The effects of each blade power variation according to AOA changing with Tip Speed Ratio (TSR) (λ) ranges from 3 to 7.5 which was analyzed thorough the understanding of the flow of hydrodynamics. The relationship between the number of blades and the tip speed ratio is influenced by the input flow conditions. The power to TSR relation is presented in Fig. 9 for 2, 3 and 4 number of blades. Specifically, a higher number of blades tend to correspond to a lower TSR. Conversely, a higher TSR leads to a reduction in the number of blades. It is observed that turbines with fewer blades generally operate efficiently at higher TSR values due to reduced drag and higher rotational speed. On the other hand, turbines with more blades produce greater torque at lower TSRs. Among the tested configurations, the 3 bladed turbine consistently exhibited the highest power output at moderate TSR values and confirms its balanced aerodynamic behavior and reduced energy losses due to wake interference.

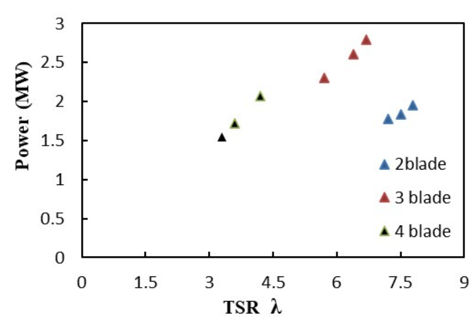

Fig. 9: Comparison of Power relation with TSR according to AOA 10, 20, 30 degrees.

b) Power- number of blades relationship: This study presents numerical data that investigate the operational efficiency of the Horizontal Axis Tidal Current Turbine (HATCT) across different turbine angles of attack (ranging from 10 to 30 degrees) and blade counts (ranging from 2 to 4). The values of these parameters were derived precisely through the utilization of the experimental model and the evaluation of the validation accuracy. The present study aims to examine the impact of individual non-dimensional features, notably the number of blades, on the efficiency of HATC turbines. The comprehensive and noteworthy discoveries on maximum power are succinctly outlined in the Fig. 10. However, beyond three blades, additional drag reduces the net energy conversion efficiency. Fig. 9 shows that the maximum power occurs for the 3-blade configuration at 30° angle of attack, validating that this combination produces the most favorable lift to drag ratio and effective utilization of the fluid kinetic energy.

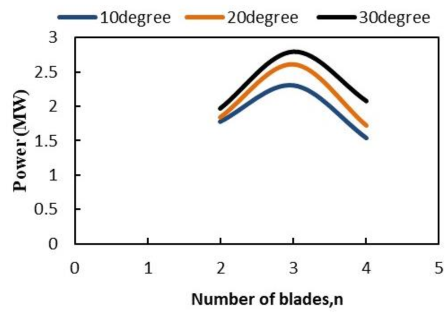

Fig. 10: Comparison of Power changing with number of blades.

c) BETZ Limit of Tidal Turbine: An assessment of the operational performance of tidal current turbines can be carried out via a methodology that is analogous to the one applied for wind turbines. Nevertheless, the characteristics of the water and the accompanying currents impose several additional factors that must be considered in the construction of these facilities. The factors encompassed in this category consist of an increased Reynold number at a given velocity, the limit of cavitation, the performance of the turbine, and the interaction between surface waves and the revolving rotor. Based on the Betz limit, it is postulated that the maximum amount of kinetic energy that can be harnessed by an ideal tidal current turbine is limited to 59.2% of the total kinetic energy of the tidal current absorbed by the turbine rotor. Which means the maximum value of C_P = 16/27 = 0.593 or 59.3% while only 70% of this flux passes through the rotor.

In this study, the maximum obtained C_p = 0.47 for the 3 bladed turbine at 30° angle of attack which is below the Betz limit but within an acceptable and realistic range for practical marine turbines. This confirms that the simulated design efficiently extracts kinetic energy without exceeding theoretical constraints. The findings from the three-dimensional analysis of optimal design indicate a significant correlation between the maximum coefficient of power (C_P) and the tip-speed ratio (TSR) when examining various turbine configurations which is exhibited from Fig. 11 for different angles of attack and blade quantities. An augmentation in turbine power and the addition of more blades lead to an elevation in coefficient of power (C_P) across the full range of the ratio of tip speed (TSR) investigated, with the highest C_P achieved at lower TSR values. Overall, the analysis establishes that both angle of attack and blade number play critical roles in determining turbine performance and their combined optimization particularly the 3 blade 30° configuration offers the best compromise between torque, power and hydrodynamic efficiency.

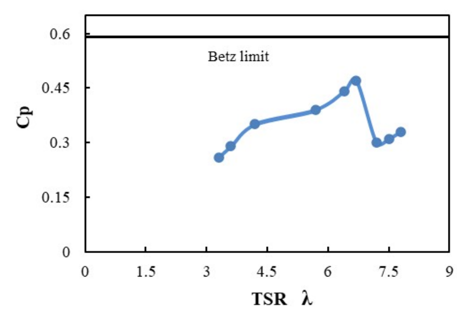

Fig. 11: Comparison with coefficient of power C_P changing with TSR and Betz limit.

Conclusions: The numerical study based on CFD of an 11.1m horizontal axis tidal turbine blade was carried out for three different angles of attack: 10°, 20°, and 30°, as well as three different numbers of blades. The turbine blades were modeled in SOLIDWORKS and simulated using ANSYS CFX to assess torque, power, and power coefficient under varying flow conditions. The findings clearly demonstrate that turbine performance improves with an increase in angle of attack up to 30°, where maximum torque and power were achieved. Among the tested configurations, the 3-bladed turbine at a 30° angle of attack yielded the highest performance, producing 2.79 MW of power with a maximum power coefficient of 0.47. This configuration provided the most effective balance between lift, drag, and torque, confirming its superiority in terms of hydrodynamic efficiency. The result substantiates the research objective of identifying an optimal design configuration for enhanced energy extraction from tidal currents. The achieved Cp value remains within realistic operational limits and below the theoretical Betz limit (0.593), verifying both the physical validity and reliability of the CFD predictions. Overall, the study establishes that careful optimization of blade geometry and operating parameters. Particularly, the combination of a three-blade configuration with a 30° angle of attack can significantly improve the energy conversion efficiency of HATCTs. Future work may explore alternative blade profiles, three-dimensional transient simulations, and real sea environmental modeling to further refine turbine performance and assess long-term operational challenges.

References:

[1] M. Nazari, Study and design of the point absorber wave energy for Persian Gulf, Master Thesis, Amirkabir University of Tech, 2011.
[2] M. Nazari, H. Ghassemi, M. Ghiasi, M. Sayehbani, Design of the point absorber wave energy converter for Assaluyeh Port, Iranian Journal of Energy and Environment, 2013.
[3] Q. K. Xu, H. W. Liu, Y. G. Lin, X. Yin, W. Li, Y. J. Gu, Development and experiment of a 60-kW horizontal-axis marine current power system, Energy, 2015.
[4] Q. Xu, W. Li, Y. Lin, H. Liu, Y. Gu, Investigation of the performance of a standalone horizontal axis tidal current turbine based on in situ experiment, Ocean Eng, 2016.
[5] Y. J. Gu, X. Yin, H. W. Liu, W. Li, Y. G. Lin, Fuzzy terminal sliding mode control for extracting maximum marine current energy, Energy, 2015.
[6] M. R. Barakat, B. Tala-Ighil, H. Chaoui, H. Gualous, Y. Slamani, D. Hissel, Energetic macroscopic representation of a marine current turbine system with loss minimization control, IEEE Trans Sustain Energy, 2018.
[7] B. Wu, X. Zhang, J. Chen, M. Xu, S. Li, G, Li, Design of high-efficient and universally applicable blades of tidal stream turbine, Energy, 2013.
[8] I. A. Milne, A. H. Day, R. N. Sharma, R. G. J. Flay, Blade loading on tidal turbines for uniform unsteady flow, Renew Energy, 2015.
[9] T. A. J. Henriques, S. C. Tedds, A. Botsari, G. Najafian, T. S. Hedges, C. J. Sutcliffe, The effects of wave current interaction on the performance of a model horizontal axis tidal turbine. Int J Marine Energy, 2014.
[10] M. J. Lewis, S. P. Neill, M. R. Hashemi, Reza M. Realistic wave conditions and their influence on quantifying the tidal stream energy resource, Appl Energy, 2014.
[11] G. W. Wu, H. Wu, X. Y. Wang, Q. W. Zhou, Liu X-m. Tidal turbine array optimization based on the discrete particle swarm algorithm, China Ocean Eng, 2018.
[12] L. E. Myers, A. S. Bahaj, Simulated electrical power potential harnessed by marine current turbine arrays in the Alderney Race, Renew Energy, 2005.
[13] L. E. Myers, A. S. Bahaj, An experimental investigation simulating flow effects in first generation marine current energy converter arrays, Renew Energy, 2012.
[14] V. Gupta, A. M. Young, A one-dimensional model for tidal array design based on three-scale dynamics, J Fluid Mech, 2017.
[15] A. S. Bahaj, A. F. Molland, J. R. Chaplin, W. M. J. Batten, Power and thrust measurements of marine current turbines under various hydrodynamic flow conditions in a cavitation tunnel and a towing tank, Renewable Energy, 2007.
[16] W. Xu, Numerical Techniques for the Design and Prediction of Performance of Marine Turbines and Propellers, Master Thesis, University of Texas at Austin, 2010.
[17] W. Shi, D. Wang, M. Atlar, K. Seo, Flow separation impacts on the hydrodynamic performance analysis of a marine current turbine using CFD, Proceedings of the Institution of Mechanical Engineers Part A Journal of Power and Energy, 2013.
[18] B. Gunawan, V. S. Neary, Model validation using experimental measurements from the Garfield Thomas water tunnel at the applied research laboratory at Penn State University, Proceedings of the 2nd Marine Energy Technology Symposium, 2014.
[19] N. G. Kai-Wern, H. L. Wei, N. G. Khai Ching, 2002–2012: 10 Years of Research Progress in Horizontal-Axis Marine Current Turbines, Energies, vol. 6, no. 3, pp. 1497-1526, 2013.
[20] E. A. Evi, R. A. Harinaldi, I. Ridho, Experimental study on the optimum design of diffuser-augmented horizontal-axis tidal turbine, Clean Energy, vol. 6, no. 5, p. 776–786, October 2022.
[21] W. Shu-Qi, Z. Ying, X. Yang-Yang, X. Gang, L. Kun, Z. Yuan, Hydrodynamic Analysis of Horizontal Axis Tidal Current Turbine under the Wave-Current Condition, Journal of Marine Science and Engineering, vol. 8, no. 8, p. 562, July 2020.
[22] I. E. Job, J. Cameron, O. S. Stephanie, Design of a Horizontal Axis Tidal Turbine for Less Energetic Current Velocity Profiles, Journal of Marine Science and Engineering, vol. 7, no. 7, p.197, 2019.
[23] A.S. Bahaj, L. E. Myers, Fundamentals applicable to the utilisation of marine current turbines for energy production, Renewable Energy, vol. 28, no. 14, pp. 2205-2211, 2003.
[24] R. Malki, M. Ian , J. W. Alison, C. Nick, Planning tidal stream turbine array layouts using a coupled blade element momentum - computational fluid dynamics model, Renewable Energy, vol. 63, pp. 46-54, 2014.
[25/12] R. H. Binoe , E. Abuan, The Performance and Hydrodynamics in Unsteady Flow of a Horizontal Axis Tidal Turbine, Renewable Energy, 2019.
[26] R. Noruzi, M. Vahidzadeh, A. Riasi, Design, analysis and predicting hydrokinetic performance of a horizontal marine current axial turbine by consideration of turbine installation depth, Ocean Engineering, 2015.
[27] V. T. Nguyen, S. S. Guillou, J. Thiebot, A. S. Cruz, Modeling turbulence with an Actuator Disk representing a tidal turbine, Renewable Energy, 2016.
[28] S. S. Kulkarni, Design study of a horizontal axis tidal turbine blade, Doctoral thesis, Birmingham City University, 2016.
[29] T. Razzak, M. N. Hussain, M. D. Hussain and M. M. Uddin, Numerical Investigation on Hydrodynamic Performance of a Horizontal Axis Tidal Current Turbine, SSRN Electronic Journal, Published by Elsevier, 2024.
[30] S.F.H. Munna, and M.M. Uddin, CFD analysis on horizontal axis tidal current turbine, Research on Engineering Structures & Materials, 2025.
[31] C. C. Chen, Y. D. Choi and H. Y. Yoon, Blade design and performance analysis on the horizontal axis tidal current turbine for low water level channel, IOP Conference Series: Materials Science and Engineering, 2013.
[32] D.P. Coiro, U. Maisto, F. Scherillo, S. Melone and F. Grasso, Horizontal Axis Tidal Current Turbine: Numerical and Experimental Investigations, Civitavecchia, Italy, *2006.*
[33] L. Yangjian, L. Hongwei, L. Yonggang, L. Wei and G. Yajing, Design and test of a 600-kW horizontal-axis tidal current turbine, Energy, 2019.
[34] K. M. Wibowo, B. Rudiyanto, Experimental study on pitch angle effects on the performance of Sg-6043 horizontal wind turbine, Journal of Physics: Conference Series, 2019.
[35] F. H. Haydar, E. S. Ahmed, O. A. Karim, Tidal current turbines glance at the past and look into future prospects in Malaysia, Renewable and Sustainable Energy Reviews, 2012.
[36] M. A. Shatter, K. A. Khan, The Prospect of Tidal Energy in Bangladesh, The Proceedings of Third International Geo-Hazards Research Symposium (IGRS), Tehri Garhwal, India, 2012.